

A Hybrid 3D Learning-and-Interaction-based Segmentation Approach Applied on CT Liver Volumes

Marius DANCIU¹, Mihaela GORDAN¹, Camelia FLOREA¹, Radu ORGHIDAN¹,
Erich SORANTIN², Aurel VLAICU¹

¹ Dept. of Communications, Technical University of Cluj-Napoca, C. Daicoviciu 15, Cluj-Napoca, Romania

² Dept. of Radiology, Medical University Graz, Auenbruggerplatz 34, Graz, Austria

{Marius.Danciu, Mihaela.Gordan, Camelia.Florea, Radu.Orghidan, Aurel.Vlaicu}@com.utcluj.ro,
Erich.Sorantin@medunigraz.at

Abstract. *Medical volume segmentation in various imaging modalities using real 3D approaches (in contrast to slice-by-slice segmentation) represents an actual trend. The increase in the acquisition resolution leads to large amount of data, requiring solutions to reduce the dimensionality of the segmentation problem. In this context, the real-time interaction with the large medical data volume represents another milestone. This paper addresses the twofold problem of the 3D segmentation applied to large data sets and also describes an intuitive neuro-fuzzy trained interaction method. We present a new hybrid semi-supervised 3D segmentation, for liver volumes obtained from computer tomography scans. This is a challenging medical volume segmentation task, due to the acquisition and inter-patient variability of the liver parenchyma. The proposed solution combines a learning-based segmentation stage (employing 3D discrete cosine transform and a probabilistic support vector machine classifier) with a post-processing stage (automatic and manual segmentation refinement). Optionally, an optimization of the segmentation can be achieved by level sets, using as initialization the segmentation provided by the learning-based solution. The supervised segmentation is applied on elementary cubes in which the CT volume is decomposed by tiling, thus ensuring a significant reduction of the data to be classified by the support vector machine into liver/not liver. On real volumes, the proposed approach provides good segmentation accuracy, with a significant reduction in the computational complexity.*

Keywords

3D liver segmentation, 3D DCT, blocks level volume segmentation, SVM, 3D human-computer interaction, segmentation refinement, 3D level set segmentation, neuro-fuzzy interaction.

1. Introduction

In the area of medical imaging, a core problem with significant impact on computer aided medical diagnosis

consists in the segmentation of the organs, leading to the delineation of the volume of interest (VOI) from the sequence of slices which form the 3D representation of the body portion scanned in different modalities. This represents the first stage in computer-aided diagnosis and surgical procedures; therefore the accuracy of the delineation is crucial for therapy. One of the often preferred medical image acquisition modalities is computer tomography (CT), due to its affordable cost and availability in many hospitals. The segmentation of various organs in CT raises particular challenges, which explains the development of different organ specific segmentation algorithms in CT volumes segmentation.

In this paper we aim to present a rather general CT volume segmentation framework, adapted however for the liver segmentation task. A study of the relevant literature reveals the fact that liver delineation from CT scans is not an easy task due to a multitude of factors, such as variations in contrast, acquisition noise, as well as inter-patient variability in the shape, size and structure (i.e., texture and intensity) of the liver parenchyma. Other difficulties in the segmentation of the liver are generated by the nearness and similarity of the surrounding organs that have the similar intensities and texture. Moreover, local variations in the intensity and texture of the same organ may appear in the CT scans, due to some pathology, to the contrast agent administered or due to the particularities of the local surrounding tissues. Even more challenges arise due to the different configurations of the CT scanners.

Recent literature presents different algorithms for liver segmentation, which can be mainly divided in three classes: automatic, semiautomatic [1] - [3], or interactive [4], [5]. Obviously, automatic liver segmentation is the preferred technique, as it saves a precious time and effort of the radiologist specialist (otherwise having to perform the segmentation manually, often slice by slice in the so-called pseudo-3D approaches), but is also the most challenging, as it should be accurate and computational effective, despite the multitude of factors which leads to a large variation of the liver in CT scans mentioned above.

A large variety of automatic liver segmentation algorithms is presented in the recent literature, differing in the

type of features used for describing the liver and in the type of knowledge implied to describe the liver shape and location. Some methods consist in a series of 2D segmentations, applied slice by slice on the CT scan and grouped in the final stage into a 3D segmentation; therefore they are often referred as “pseudo-3D”. Such methods are often not fully able to exploit the 3D correlations of voxels composing the medical volume. Therefore the preferred trend is the development of full 3D segmentation procedures, by extending the 2D segmentations schemes on volume data. Different classes of automatic CT liver segmentation methods are reported. The simplest category involves threshold [6] or multi-threshold [7] segmentation applied on the intensity only. The segmentation accuracy achieved by this strategy is rather low, as the intensities inside the liver are neither always homogeneous, neither perfectly discriminative between the liver and other organs. A better strategy is to take into account also the texture information as significant segmentation feature. A recent survey on texture analysis for liver segmentation can be found in [8]. The most commonly used texture descriptors for liver include the gray level difference statistics (GLDS), gray level run length statistics (RUNL), edge frequency based texture features, Laws texture energy measure (TEM), as well as transform based features: Fourier Power Spectrum (FPS), Wavelet features, Discrete Cosine Transform (DCT) features. These features are further used in different segmentation framework, many of which involve the classification of the pixels (in the case of slice-by-slice segmentation of the CT volume) or voxels (in the case of a real 3D segmentation) by either supervised or non-supervised classifiers to achieve the delineation of the liver.

The prior knowledge based approaches represent another appealing category for liver segmentation. The association between topological distance and orientation is used as prior knowledge in [9]. Another recent class of algorithms is oriented on atlas-guided segmentation [10], [11]. In the statistical approaches, a statistical model discrimination of the liver is established from quantities of data sets [12], but in general, the model generation is time consuming and requires a large amount of information to be able to adapt to inter-patient variability. Another significant set of CT medical image segmentation approaches is based on active contour models [13], [14], fast marching [15] and level set method [16]; however it should be noted that the success of these methods depends significantly on the initial estimate of the shape of the organ, which should be roughly accurate for a fast convergence and good accuracy of the final segmentation.

Despite the wide range, mathematically complex and rigorous algorithms and constant improvements in the automatic segmentation approaches, the fully automated segmentation results are still prone to errors and flaws. These flaws are often locally bound, such as – in case of the liver – leakage into the heart and stomach region, or problems with vena cava inferior. These observations have led researchers and radiology specialists to believe that computer-aided interactive editing of the segmented sur-

face generated by an automatic algorithm – *segmentation refinement* – is a suitable compromise, which is much less time consuming than manual segmentation, yet yields high quality results directly usable in surgery planning.

The traditional interaction devices, offering clinicians the possibility to edit volumetric medical data slice by slice, are no longer satisfactory, considering that in daily practice, 3D anatomical objects are mentally reconstructed – as a natural cognitive ability of humans. Since nowadays software applications provide 3D reconstruction of anatomical structures facilities, augmented and virtual reality offer a more natural way of evaluating the segmentation results, facilitating diagnosis. Immersive interaction techniques can also be used for increasing real space perception of medical data. Following these considerations, it is important to have 3D interaction techniques to manipulate virtual representations of human organs, and this is currently an emerging medical imaging field. According to Bowman et al. [2], 3D interaction should be defined as the type of human-computer interaction in which user’s tasks are done in a 3D context – therefore simple non-obstructive interfaces are required.

Many research teams investigated and developed new interaction and visualization modalities – some of them specifically designed for medical applications. Gratzel et al. [17] presented a non-contact mouse for surgeon – computer interaction using gestures. Feied et al. [18] also developed a hands-free system for visualization of medical images during clinical procedures, to avoid radiologists’ contact with the keyboard and the mouse, as potential contamination sources. De Paolis et al. [19] propose another system that helps surgeons to model patient’s organs and interact with them in a more effective way for pre-operative planning and also during the real surgical procedure. The finger movements are detected by means of an optical tracking system and are used to simulate the touch of the virtual interface. Gallo and Ciampi [20] developed a 3D interface for medical data exploration. 3D medical data can be manipulated in a semi-immersive virtual environment using a data glove with an attached infrared led, tracked by a Wii remote sensor. Another medical data visualization system is proposed by Cooperstock and Wang [21], which implements interaction techniques similar to the manipulation of physical objects. Reitingner et al. [22] developed a system for planning liver surgical procedures, called LiverPlanner, with the benefits of stereoscopic visualization through HMD and 3D interaction for refinement of medical images through a system that tracks both the body position and the interaction device using an optical tracking system. The manual segmentation refinement approach employed in the proposed system represents a flexible, computationally efficient solution implementing a virtual probe for 3D volumes interaction, where the positioning is based on a neuro-fuzzy algorithm.

The segmentation framework that we propose in this paper provides not only an accurate and flexible 3D segmentation solution, but also a numerical efficient one, as it

generalizes the 2D DCT based compressed domain image segmentation (proven more efficient than the pixel segmentation in the case of JPEG image encoding [23]) for the 3D case. The proposed supervised liver segmentation method can successfully outline liver in 3D abdominal volumes (CT slices), and when it is combined with manual refinement facilities and level sets methods, the accuracy can be increased even further. Its main novelty is the derivation of the local features in medical volume data based on a 3D DCT decomposition applied on voxels blocks. For the decision on the resulting 3D blocks (as belonging or not to the liver) we employ a probabilistic support vector machine (SVM) classifier. The SVM segmentation result is refined by several 3D post-processing operations (filtering, morphological operations, connected components analysis) applied on the intermediate probabilistic output of the SVM classifier. Furthermore, the subsequent 3D interaction system for medical volume editing allows an interactive correction/refinement of automatic segmented volume. Thus the proposed approach provides a complete 3D solution to medical volumes segmentation, as illustrated on CT images for liver segmentation, where it provides higher accuracy than some state of the art solutions, at lower computational complexity cost.

The remaining of the paper is structured as follows: Section 2 represents schematically all the steps involved in the segmentation process. Section 3 describes in detail the supervised segmentation stage of the proposed 3D segmentation method. Section 4 presents the proposed solution for 3D volume interaction and editing, used in this case for rough segmentation refinement. In Section 5, the experimental results are presented, and finally, Section 6 presents some conclusions and possible future extensions of our work.

2. General Structure of the Hybrid 3D Learning-and-Interaction Segmentation System

Current automatic segmentation approaches for soft tissue organs are most of the time focused on a specific problem. Some organs like the heart can be segmented using model-based approaches, since the degree of shape variation is rather low. For organs with a high degree of shape variation, **liver case**, such approaches may fail, and segmentation algorithms have to rely on information available in images such as gray value and gradient information. Unfortunately, the required information cannot always be extracted from the images using common approaches, as in the case of adjacent organs that share the same gray values in the CT image. The resulting incorrect segmentation cannot be used in preoperative planning, and therefore the medical personal have to rely on manual segmentation by drawing segmentation outlines in each 2D image of the volumetric set. This procedure is time consuming and inefficient for high resolution scans with hundreds of slices. Moreover, even trained radiologists tend to misinterpret complex 3D anatomy when only viewing 2D cross-sections. It must be highlighted that automatic segmentation algorithms can successfully accomplish the recovering of major parts of the targeted organs structure in many medical applications including liver segmentation.

Therefore, we propose a new computationally efficient three step solution for 3D liver segmentation (see Fig. 1.). The first step implies a 3D automatic segmentation, based on support vector machine classification of volume blocks described by the 3D DCT blocks. The segmentation result is refined by post-processing: 3D median

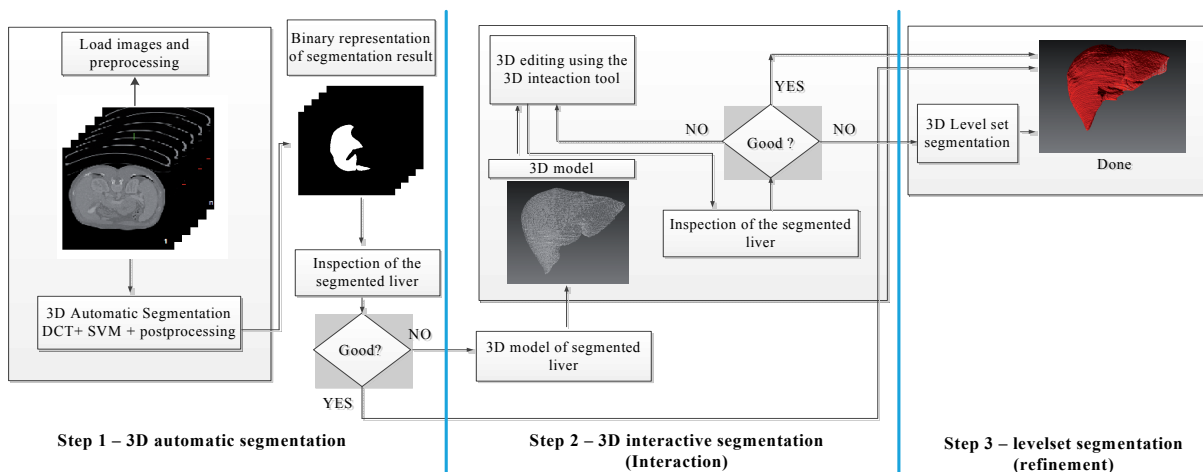


Fig. 1. The main three steps for the segmentation process.

filtering, 3D morphological operations, and 3D connected components analysis.

In the second step a 3D interactive segmentation (interaction tools) integrates several functionalities to medical volume editing and visualization: 3D measurements; posi-

tioning arbitrary cutting planes; cropping a volume of interest; surface/volume smoothing; 3D morphological operations; anaglyph stereo visualization. Its main novelty is the use of fuzzy logic in the 3D virtual probe positioning, with the advantages of a low memory usage, real-time

operation and low positioning errors as compared to classical solutions. These tools are easy to manipulate and allow a high positioning precision during the interaction with the virtual medical volume.

The third step, level set segmentation, is used for segmented volume final refinement, based on active contours.

In the third step, level set segmentation is used for the final refinement of the segmented volume; to preserve the benefit of the fast computations ensured by our solution, we chose to employ a fast approximation of the zero level set method developed by Malcolm et al. [24]. Provided a good initialization is available, as offered by our system, the level set method has already proven very successful in medical volumes segmentation (and there are several works using this strategy as a kind of “last post-processing” step, for refining the segmentation results in the last decade, e.g. Jiang et al. [25]).

3. 3D DCT Supervised Segmentation Component

The 3D automatic segmentation process is described in Fig. 2. The segmentation approach contains two phases: the training phase and the testing phase. The feature vector is formed by the quantized 3D DCT coefficients and for data classification a support vector machine is used. Here, the DCT is applied locally, on block level, following the image/volume splitting into square/cube blocks.

We consider the 3D volumes divided in non-overlapping blocks (by tiling), for two main reasons. The algorithm is not applied on each pixel, but on each non-overlapping block, not just for reduce the computational complexity, but also to open the direction of developing this algorithm directly in the compressed domain. Nowadays, in order to save storage space and time for data transmission, even the medical images are compressed. The most used compression standards are the ones based on DCT, among JPEG is widely used. For store the CT volumes each image slide is independently compressed.

In the JPEG compression standard the image is first divided into 2D blocks of 8×8 pixels and each block is compressed individually [26]. In our segmentation method, we use blocks of 4×4 pixels, which can be extracted directly in the compressed domain by using the relationship between a 2D DCT block and its 2D DCT sub-blocks [27] (this implies three sparse matrices multiplications). For CT volumes, compressed in the JPEG format, the 3D DCT blocks can be obtained, without decompression, by applying the 1D DCT on a set of image slides. Therefore, the compressed domain implementation seems to be feasible, offering a significant computational time reduction that is a very important aspect when dealing with 3D volumes.

For segmentation, the feature vector is formed by the quantized 3D DCT coefficients. The 3D blocks of the DCT

coefficients are ordered in a manner that indicates the frequency components in an ascending order, therefore, the biggest (which are the most relevant) values are grouped at the beginning of this vector. Due to quantization a large amount of the DCT coefficients are zero (many of the AC coefficients, usually the high frequency ones, are quantized to zero), therefore part of the values are not included in the feature vector.

The SVM segmentation result is followed by a 3D post-processing.

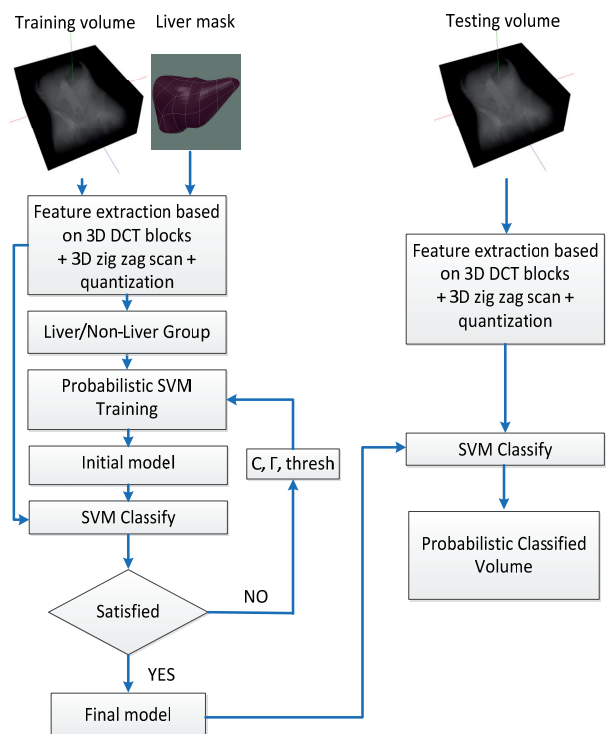


Fig. 2. The 3D automatic segmentation process.

3.1 3D DCT Features Extraction

The discrete cosine transform (DCT) is widely used in image segmentation/classification and compression, due to its properties: the data de-correlation and efficient energy compaction. The DCT image representation concentrates the spatial content in relatively few non-zero coefficients. The DCT coefficients contain many features about the content of image, reflecting the same features as those used at pixel level. Thus, the DC coefficient represents the average intensity value in a block of pixels/voxels, while the AC coefficients reflect the variance of luminance changes in pixels/voxels within the same block.

The DCT is considered one of the best options for textural feature extraction, therefore, the use of DCT coefficients in texture-based image segmentation/ classification has been explored by several researchers [23], [28]. The DCT based approaches can outperform the discrete Wavelet transform (DWT) ones, if a compromise efficiency-accuracy is considered [28].

The DCT is also used in popular compression standards such as JPEG and MPEG. Nowadays, 3D DCT is considered as a solution for three dimensional image compressions [29]. There are several 3D DCT based techniques to compress video sequences, multi-view image sets and other types of stereoscopic data.

Image segmentation can be done on pixel/voxel level considering the local color and texture information, but also at block level in the reduced feature space formed by the ordered quantized DCT coefficients.

Taking into account the success of the existing approaches of texture segmentation directly in the quantized DCT coefficients domain [23] (mainly implemented on JPEG images and MPEG video sequences), with their computational efficiency advantage, we propose a 3D DCT block level segmentation. Our approach splits the 3D volume into non-overlapping blocks of size $N \times N \times N$ (where N is small enough to approximate accurately a unit volume, but large enough to capture local texture properties in the volume; e.g. $N = 3 \dots 8$). For each block the ordered quantized 3D DCT coefficients are computed and arranged in vector form, thus representing each unit volume from the liver in a feature space whose dimension is significantly smaller than $3N$ (due to the coefficients quantization). Therefore the entire volume is represented by a set of data that is N^3 times smaller than the original number of voxels. The reduced feature space, as well as the reduced data set, makes the implementation of rather complex segmentation procedures computationally easier.

The 3-D DCT of each $N \times N \times N$ voxels block, described by the intensity values in the spatial locations (x, y, z) in the block ($\mathbf{f}(x, y, z)$ – the intensity value) is defined as:

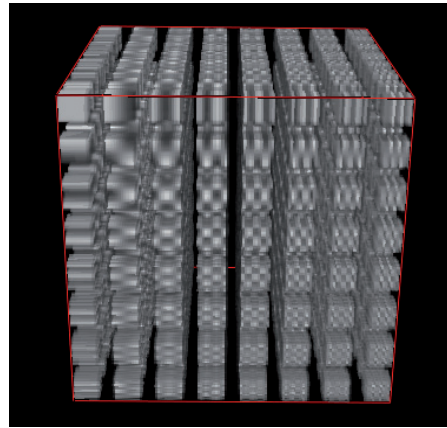
$$\mathbf{F}(u, v, w) = \sum_{x=0}^{N-1} \sum_{y=0}^{N-1} \sum_{z=0}^{N-1} \mathbf{f}(x, y, z) \mathbf{C}(x, u) \mathbf{C}(y, v) \mathbf{C}(z, w), \quad (1)$$

$$\text{where: } \mathbf{C}(p, q) = \begin{cases} \frac{1}{\sqrt{N}}, & q = 0 \\ \sqrt{\frac{2}{N}} \cos\left(\frac{(2p+1)q\pi}{2N}\right), & q \neq 0 \end{cases}$$

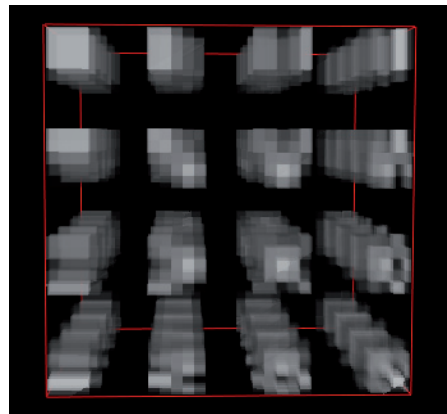
and $\mathbf{F}[N \times N \times N]$ is the 3D DCT coefficients block, with $\mathbf{F}(u, v, w)$ representing the value of a DCT coefficient.

The $8 \times 8 \times 8$ DCT basic volumes are represented in Fig. 3.(a), together with the proposed approach that uses only a variant of $4 \times 4 \times 4$ DCT basic volumes in Fig. 3(b).

The dominant AC coefficients spread along the major axes of the 3D-DCT cube [30]. The coefficient distribution can be modeled by splitting the cube into two regions: the left-upper region which will include the most significant coefficients and the right-down region which will include the high frequency coefficients (these are very low values or zero and can be eliminated, as most of them account for noise).



(a)



(b)

Fig. 3. (a) Basic $8 \times 8 \times 8$ DCT volumes, (b) Basic $4 \times 4 \times 4$ DCT volumes.

In this paper, the quantization is done by eliminating the values from the second region and rounding the DCT coefficients from the first region to the nearest integer. In this step the redundant information is eliminated.

To determine the optimal truncation order of the 3D-DCT coefficients for the given liver segmentation problem, we implemented the two most familiar approaches [30]: a linear 3D zigzag scanning (using the isoplane) and a shifted complement hyperboloid function.

In the first approach, the linear 3D zig-zag scanning, the 3D DCT coefficients are ordered based on the sum of their indices:

$$\mathbf{g}(u, v, w) = u + v + w \leq K \quad (2)$$

where the function $\mathbf{g}(u, v, w)$ defines the left-upper region (as shown in Fig. 4. by blue color/ solid area) and represents the position of the quantized $\mathbf{F}(u, v, w)$ DCT coefficients that are included in the feature vector.

The border (as illustrated in Fig. 4(a)) between the two regions (the dominant and the less significant coefficients, respectively) is controlled by the constant value K . However, this approach doesn't include effectively the 3D DCT coefficients along the major axes and it includes more zeros inside the cube.

In the second approach, the shifted complement hyperboloid function was used to select the dominant 3D DCT coefficients as illustrated in Fig. 4(b). This approach is better than the linear 3D zig-zag scan method in general, since it includes effectively the 3D DCT coefficients along the major axes and it includes less zeros inside the cube. The shifted complement hyperboloid function is defined as:

$$g(u, v, w) = u \cdot v \cdot w \leq K \quad (3)$$

where K is a positive real-valued scalar controlling the amount of 3D DCT coefficients to be kept after the truncation.

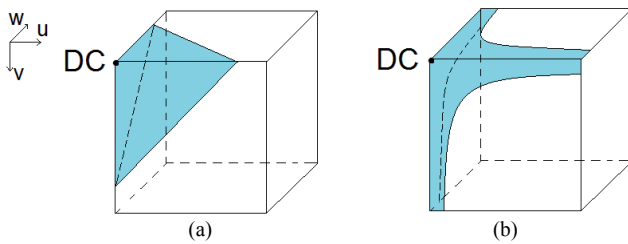


Fig. 4. (a) The linear 3D zigzag scanning, (b) The region defined by a shifted complement hyperboloid function.

In our segmentation approach, the ordered quantized 3D DCT coefficients that represent essential features (in a reduced data space - the majority of the AC coefficients are zero after the quantization) are used in the next step for data classification by SVM in either “liver blocks” or “non-liver blocks”. Therefore, we benefit of the major advantage of obtaining a reduced computational complexity while preserving all the data needed for an accurate classification.

3.2 Support Vector Machine Classification

Support vector machines (SVMs) are one of the most popular machine learning methods in classification and regression [31]. In its implicit form, an SVM is a binary classifier which provides the benefit of learning with high precision and recall from a relatively sparse set of training data. The segmentation problem addressed here can easily be regarded as a binary classification of the elementary volume blocks in one of two classes: liver or non-liver, therefore the use of a binary SVM classifier for this task in the feature space described in the previous sub-section is a suitable and appealing solution.

The SVM classification principle lies in the derivation of an optimal separating hyperplane that will classify the data from the two classes associated to the binary classification problem with – ideally – no error and with maximum margin to the hyperplane for the data in both classes. The derivation of the optimal separating hyperplane is done in the training phase, based on a set of labeled training data. In the classification phase, the position of any unlabeled data in respect to the hyperplane determines the classification of the data. Of course, depending on the classification problem and on the feature space, the data

may be or may not be linearly separable. In the case of linearly separable data, a linear SVM would perform very well; however in the most frequent case of non-linearly separable data, one can use a non-linear SVM classifier. In principle a non-linear SVM classifier projects the data from the original feature space in a higher dimensional feature space, through the use of some kernel mapping, in which the data become linearly separable. Then the optimal separating hyperplane is derived in this higher-dimensional feature space, and further used for classification.

Among the most familiar kernel functions, the polynomial kernels and radial basis function (RBF) kernels should be mentioned.

After some preliminary tests for classification of data in liver/non-liver classes, we chose the RBF kernel as giving the best accuracy and generalization performance on a validation data set. We tune the RBF kernel parameter and the penalty factor C to minimize the error in the training set and to maximize the recall performance. For that we used a “greed-search” on C and using cross-validation.

In the most common form, an SVM classifier outputs only the most likely class label based on the principle of the position of the data versus the hyperplane. However, probabilistic extensions of SVMs exist and are very appealing [32], since they may increase the classification accuracy if combined with other post-classification refinement strategies or if the probabilistic threshold is adapted to the given data set [33] (as the default probabilistic threshold of 0.5 is not always Bayes optimal).

This probabilistic threshold = cut-off point could be found using receiver operating characteristic (ROC) curves.

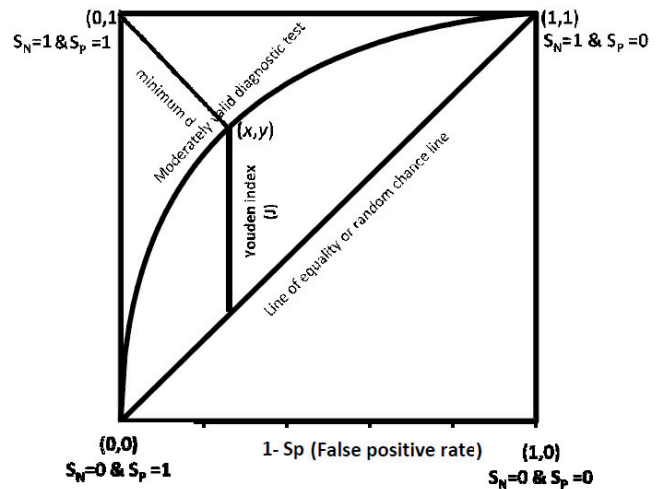


Fig. 5. Finding the best cut-off point from the ROC curve.

If S_n and S_p denote sensitivity and specificity, respectively, the distance between the point $(0, 1)$ and any point on the ROC curve is:

$$d = \sqrt{(1 - S_n)^2 + (1 - S_p)^2} \quad (4)$$

To obtain the optimal cut-off point (threshold) to discriminate the liver voxels from non-liver ones, one has to calculate this distance for each observed cut-off point, and locate the point where the distance is minimal.

3.3 3D Post-processing of the SVM Segmentation Result

The SVM classifier is able to distinguish well between the blocks with liver-like texture and other textures, but this type of texture is not specific to the liver only in an abdominal CT scan, being found in other organs as well (e.g. spleen).

Therefore misclassified blocks appear mostly outside the liver. Also some volume units inside the liver may be misclassified as non-liver, depending on the quality of the acquired volume. To improve the segmentation result, several refinement operations are employed, applied again at block level, in the sequence shown in Fig. 6.

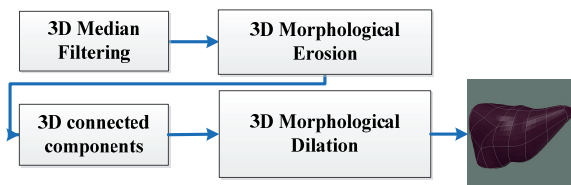


Fig. 6. Refinement process – refined segmented volume.

In order to remove blocks incorrectly classified as liver from the final segmentation, as they belong to other organs, but they share to some texture with the liver, we should use a 3D connected component labeling, which will be able to distinguish the liver if it does not appear very close to other such organs. However as the block level operation and possible misclassifications cannot guarantee this assumption (i.e. no spurious connections between the liver and another organ) in all the volumes, we perform 3D morphological erosion with a spherical structuring element prior to the connected component analysis step. This will remove the spurious connections only and not affect significantly the liver parts. Afterwards, we extract the largest component, because we know liver is the biggest component from the classified volume. To restore the size of the liver (as it was reduced due to the previous 3D erosion), a 3D binary dilation with the same spherical structuring element is applied on the extracted component.

4. The 3D Interaction-based Rough Segmentation Refinement

Immersive interaction techniques alleviate many interpretation and visualization problems and enable the clinicians to have a more intuitive image of the 3D medical data. Our goal was to design and implement a flexible, fast and accurate alternative to the few existing solutions, by integrating a neuro-fuzzy logic system in the 3D reconstruction of the virtual interaction probe.

For this purpose we developed an interaction pen-like device tracked by two web cameras, integrated with a system for 3D medical data manipulation and 3D editing. The integrated setup presents various functions for 3D segmentation refinement and for manipulation of 3D medical data [34], and the system is presented in Fig. 7.

Generally, a 3D interaction system implies the camera calibration, followed by the detection and tracking of an interaction device.

In our case, two off the shelf web-cameras are involved. A checker-board calibration pattern is used for producing a reliable training set. The input-output data must cover all the input variable space, represented as a virtual bounding box.

The method finds a set of rules defining the functionality of the cameras involved in the stereo configuration. Three fuzzy logic systems are involved, one for each dimension of the 3D space. All these fuzzy logic systems take as inputs the coordinates of the two 2D cameras: $x_i^{C_1}, y_i^{C_1}$ and $x_i^{C_2}, y_i^{C_2}$. The outputs of the fuzzy systems are the coordinates of the reconstructed points in 3D space: x_i^{3D} - on X, y_i^{3D} - on Y, and z_i^{3D} - on Z. To improve the accuracy, the initial fuzzy system is trained using an adaptive neuro-fuzzy training method (ANFIS) and the training data set. During the training, both types of fuzzy system parameters (nonlinear and linear ones) are adapted. ANFIS uses a combination of least-squares and back-propagation gradient descent methods.

The resulting fuzzy model is tested from the accuracy point of view. If the model accuracy is acceptable, the modeling procedure stops and provides the desired neuro-fuzzy model. If this is not the case, the procedure can be resumed either by re-training the fuzzy system with different parameters of the training procedure (e.g. an increased number of training epochs), generating a new initial fuzzy system with a different structure, or even by determining a new data set.

The proposed neuro-fuzzy 3D visual interaction framework integrates several functionalities to medical volume editing and visualization: 3D measurements; positioning arbitrary cutting planes; cropping a volume of interest; surface/volume smoothing; 3D morphological operations; anaglyph stereo visualization.

In order to smooth the surface of segmented liver and also to correct small misclassified voxels, we further offer the possibility of applying a final refinement approach that can be obtained with the help of deformable 3D surfaces.

The level set methods are an appealing class of deformable surface methods (more precisely, evolving surfaces as a result to some velocity fields depending on the image structure and geometry, fields that can be defined by the user), since, unlike the active surface models, they allow tracking a “boundary” surface even if the surface changes its topology. This is made mathematically possible by the introduction of a new dimension to the space where

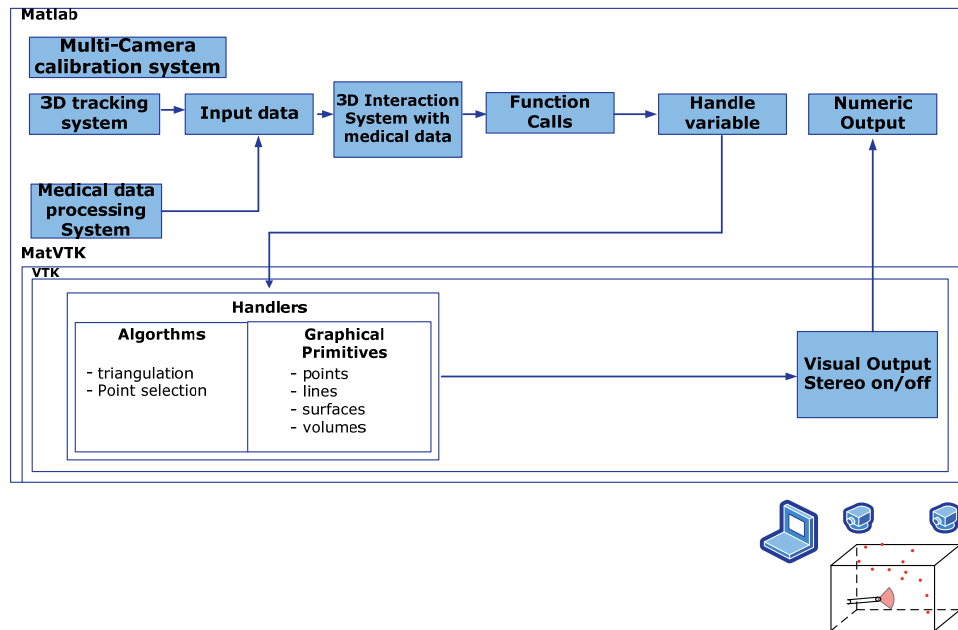


Fig. 7. Integrated system architecture for visualization and 3D interaction.

the surface lies, and defining therefore a higher dimensional, time evolving function (a surface in the higher dimensional space) whose level set is the desired boundary surface. The level set is merely the intersection of the high dimensional time evolving function with a plane. In most of the cases, only the zero level set (i.e., the intersection or the cut of the high dimensional surface with the plane passing through zero) is of interest, therefore the name of zero level set method for many level set segmentation approaches. One of the drawbacks of the level set methods in their practical applications is however their numerical complexity, which explained the development of simpler approximate implementations. Since here we only use a level set method as a segmentation refinement step, we will not proceed in detailing the mathematics behind level sets.

Following the current trend in medical volumes segmentation, we resort in this final stage to an approximation of the zero level set segmentation method, as proposed by Malcolm et al. [24]. The initial boundary surface (called in [24], interface) is provided in discrete form by the 3D liver delineation obtained after SVM classification and (if necessary) manual segmentation refinement. The volume to be segmented is re-scaled original CT liver volume. As energy term to generate the force (used to move the high dimensional surface whose zero level set is searched for), we use the mean and variance, as defined in [24], as it is proven to give the best accuracy for the set of volumes used in our experiments. It is worth mentioning that our solution already provides, as proven in the next section, a good initial estimate of the liver delineation.

Since the current segmentation result provides a very close solution to the real delineation of the liver (with possible jags however, due to the cube level segmentation of

the abdominal volume), the refinement resulting from the level set based method is expected superior to an atlas-based or manual (rough) initialization, in many cases, as the results also prove. This also explains the fast convergence of the level set and the extremely small risk of the surface being trapped in a wrong local minimum. From the many existing implementations of the level set methods for medical volume segmentation, we chose to use the approximate solution in [24] due to its reduced computational complexity, which is a requirement for practical medical volume segmentation systems, if they are to be used in assisted liver surgery.

5. Implementation and Results

The algorithm was implemented in Matlab, using an open source software LIBSVM [35] for the implementation of the probabilistic SVM, on an I5 (2.5 GHz) processor and 4 GB of memory. For the segmentation refinement by the approximate level set method, we used the Matlab package of Malcolm et al. [24], available on http://jgmalcolm.com/code/l_s_sparse.zip. Estimating processing time for volume segmentation (more than 200 slices) is about 10 minutes, which can be considered fast as compared to most reported algorithms.

Data sets used in the segmentation process are real CT slices (anonymized), each set (two data sets were used for training and 7 data sets for testing, a total of 9 datasets were involved) having between 200-350 slices. For these datasets, pixel spacing varies between 0.5-0.8 mm in x/y directions and distance between consecutive slices varies from 0.5 to 1 mm. Data set used for testing contains both types of images (with/without contrast agent), making the

segmentation process even harder. Two data sets were provided by physician Prof. Doctor Erich Sorantin (coauthor of this article) and the rest of them from MICCAI database [10]. The datasets used are shown in Tab. 1.

Volume	Pixel Dimensions	Dimensions	Contrast Agent	Data Source
1	[0.74;0.74;0.74]	[512,512,281]	yes	MICCAI
2	[0.54;0.54;0.54]	[512,512,277]	yes	MICCAI
3	[0.56;0.56;0.562]	[512,512,318]	yes	MICCAI
4	[0.69;0.69;0.69]	[512,512,315]	yes	MICCAI
5	[0.68;0.68;0.68]	[512,512,354]	no	MICCAI
6	[0.58;0.58;1]	[512,512,191]	no	MICCAI
7	[0.70;0.70;1]	[512,512,212]	yes	MICCAI
8	[0.75;0.75;0.75]	[512,512,312]	yes	Sorantin
9	[0.62;0.62;0.62]	[512,512,305]	yes	Sorantin

Tab. 1. Datasets details.

The proposed liver segmentation method has been evaluated by comparing the segmented liver to the ground truth provided by a radiologist/MICAI database. During the segmentation process we use no assumptions about size, location, and intensity range of liver, but clearly such information could further improve the segmentation.

In the preprocessing step (applied to both training and test dataset), images are resampled to isotropic voxels (using trilinear interpolation) and at the end of the segmentation process the test datasets are resampled back to the original dimensions.

The segmentation process begins with decomposition of the medical volume in blocks of 4×4×4 pixels. We choose these dimensions for our 3D data blocks because bigger blocks will lead to a much rougher segmentation. This step is followed by the application of the 3D DCT on each block and the quantization of the resulting coefficients – in our approach, simply a truncation with the shifted complement hyperboloid function Fig. 4.b, with the parameter controlling the shape of the hyperboloid (see equation (3)), $K = 3$. As the result, instead of using all 64 features that are present in a 3D DCT block, we use only 19 coefficients from each block in the process of training/classification.

The SVM kernel parameters and the optimal threshold on the SVM output probability are also adjusted based on a training/validation data set and also using ROC curves. The cut-off point (on a test dataset) using ROC curves can be observed in Fig. 8.

The performance, based on Bayes theorem, on segmentation test-set represented as a Partest graph and Roseplot Partest graph can be observed in Fig. 9.

The optimal threshold for SVM classification (in conjunction with the segmentation refinement) for the most accurate liver segmentation is found to be around 0.72.

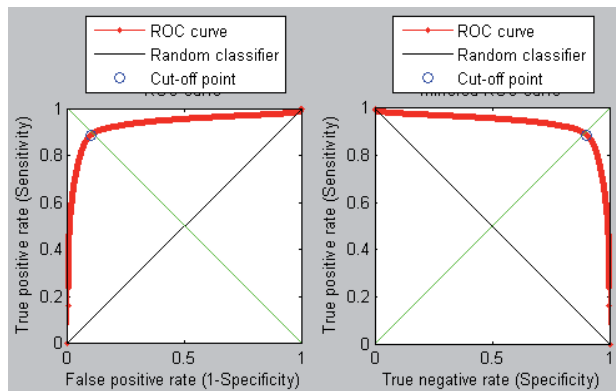


Fig. 8. Cut-off point.

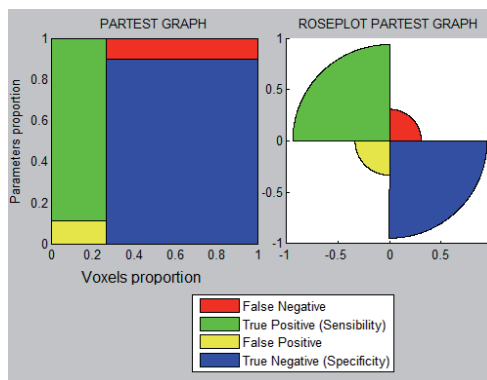


Fig. 9. Segmentation performance: Partest Graph and Roseplot Partest Graph.

In respect to the post-processing applied in the segmentation refinement, we should mention that the 3D median filter was applied in 5 by 5 by 5 neighborhoods. For the 3D morphological operations, the chosen spherical structuring element radius was 6. These parameters should be in general adapted to the acquisition device parameters.

Evaluation of the proposed algorithm was performed by computing the following parameters: sensitivity (S_n), specificity (S_p), error rate (E_r), volumetric overlap error (VO_E), accuracy (A_{cc}) and volumetric difference ($Diff_r$), defined as:

$$S_n = \frac{TP}{TP+FN}, \quad S_p = \frac{TN}{TN+FP}, \quad (5)$$

$$VO_E = 100 - \frac{V(A) \cap V(R)}{V(A) \cup V(R)} \cdot 100, \quad Diff_r = \frac{V(A) - V(R)}{V(R)} \cdot 100, \quad (6)$$

$$E_r = \frac{FP+FN}{TP+TN+FP+FN}, \quad A_{cc} = \frac{TP+TN}{TP+TN+FP+FN}, \quad (7)$$

where: TP - true positive, TN - true negative, FP - false positive, FN - false negative, $V(A)$ - segmented volume, $V(R)$ - ground truth volume.

Some of the results we obtained are shown in Tab. 2.

It is very difficult to make an objective comparison among different proposed systems due to the lack of a gold standard dataset and because every researcher uses different evaluation measures. However, some recent reported

Contrast agent	Vol	S_n	S_p	Error Rate	Acc	$Diff_V$	VO_E
no	1	0.94	0.99	1.38%	99.1%	3.7	13.1%
no	2	0.90	0.99	0.8%	99.72%	-4.5	13.56%
no	3	0.90	0.99	0.71%	99.61%	0.88	13.87%
yes	4	0.94	0.99	0.74%	99.45%	7.63	15.02%
yes	5	0.90	0.99	0.69%	99.77%	-4.8	12.83%
yes	6	0.95	0.99	0.61%	99.61%	3.64	14.08%
yes	7	0.90	0.99	0.8%	99.53%	-5.2	14.47%
yes	8	0.90	0.99	0.56%	99.90%	-7	11.96%
yes	9	0.79	0.99	1.01%	99.81%	-16.24	24.1%

Tab. 2. Segmentation evaluation.

results are the following: in [36] Ciecholewski et al. reported the sensitivity of their method to be 0.733, its specificity to be 0.833, and accuracy to be 78.3%. In [37] Campadelli et al. reported sensitivity 0.93 and 0.88 for two proposed methods for liver segmentation. In [38] Xu et al. proposed a method to segment organs including liver, and their reported sensitivity and specificity was 0.73 and 0.95 respectively. In a recent work [39] Foruzan et al. reported sensitivity, specificity, accuracy and error rate as 0.88, 0.99, 98% and 1.15% respectively.

In [40], the reported volumetric overlap error is between 14.31%–26.26%.

The approach based on wavelets proposed by [41] achieved at most 0.94 true positive (sensitivity) on test data sets, and 0.96 on partly trained data set.

Our algorithm performs better or at least with comparable results as can be seen in Tab. 1. Some segmentation examples are shown in Fig. 10, Fig. 11 and Fig. 12:

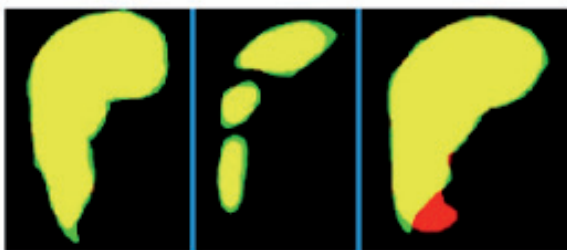


Fig. 10. Liver segmentation results: yellow – perfect segmentation, green – under-segmentation, red – over-segmentation.

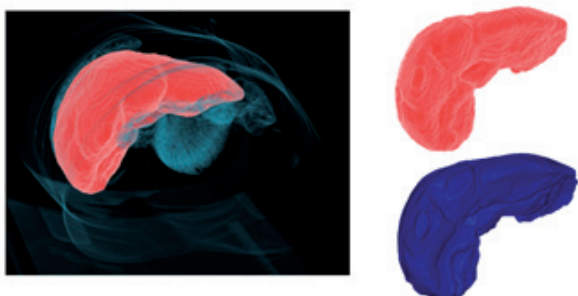


Fig. 11. 3D segmented liver relative to the abdominal cavity, 3D liver segmentation result - red, and ground truth – blue.

The hardware setup used for interaction involves a laptop equipped with an Intel i5 processor, 4 GB DDR3,

NvidiaGforce GTS 360M video graphics, one additional monitor, anaglyph glasses, two Logitech Pro 9000 webcams and the 3D interaction tool (a stick with an infrared led of 120° radiation angle attached). The system’s setup during the operation is shown in Fig. 13.

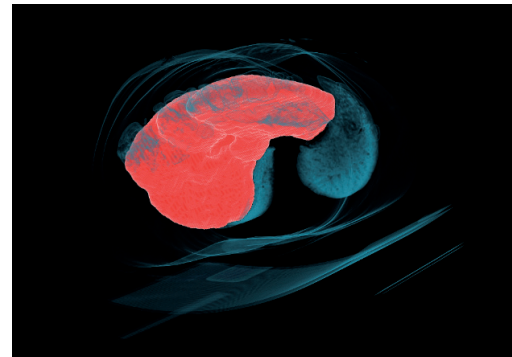


Fig. 12. 3D segmented liver relative to the abdominal cavity.

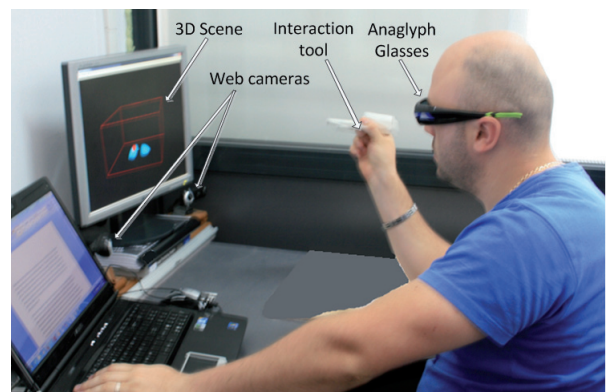


Fig. 13. The setup of the proposed 3D medical visual interaction system.

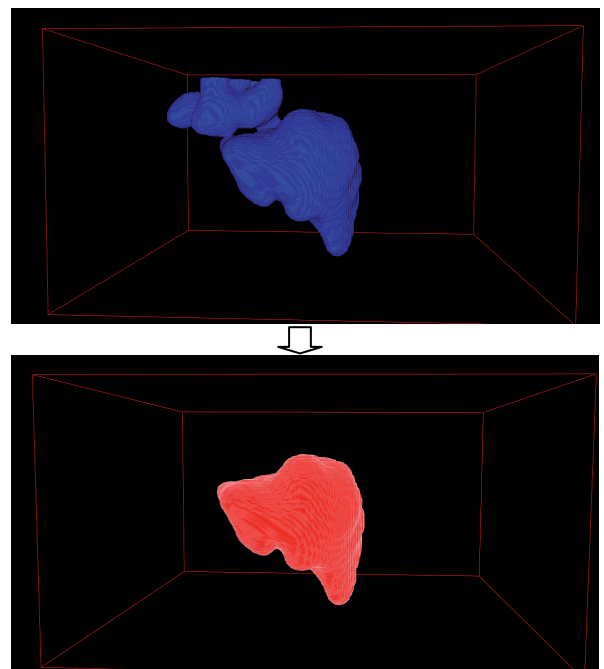


Fig. 14. Liver segmented that present leakages into the heart, and the result after segmentation refinement.

In certain cases defects appear at fully automated segmentation. These defects are often locally bound, such as – in case of the liver – leakage into the heart and problems with vena cava inferior. For such cases, editing/removing operations of these artifacts are necessary. These operations can easily be done with the help of a 3D interaction tool instead of 2D approaches that model a 3D interaction. Such an example is presented in Fig. 14 together with the applied refinement realizes with adequate interaction tools as the given one.

Results obtained after rough segmentation on different volumes are presented in Tab. 3.

Contrast agent	Vol	<i>Sn</i>	<i>Sp</i>	Error Rate	<i>Acc</i>	<i>Diff_V</i>	<i>VO_E</i>
no	1	0.95	0.99	1.2%	99.3%	2.3	12.1%
no	2	0.93	0.99	0.81%	99.80%	-2.3	11.33%
no	3	0.91	0.99	0.56%	99.81%	-4.2	11.38%
yes	4	0.95	0.99	0.67%	99.53%	5.8	13.80%
yes	5	0.91	0.99	0.72%	99.80%	-4.1	12.43%
yes	6	0.94	0.99	0.56%	99.75%	-1.67	13.13%
yes	7	0.92	0.99	0.67%	99.67%	-0.37	13.47%
yes	8	0.91	0.99	0.55%	99.87%	-6.6	11.81%
yes	9	0.89	0.99	0.58%	99.82%	-5.8	13.81%

Tab. 3. Segmentation evaluation after refinement with the interaction tool.

In order to further smooth the surface of segmented liver and also to correct small misclassified we applied 3D level set method on the results obtained at the previous step, Tab. 3. Visual results of this approach can be observed on a test slice in Fig. 15.

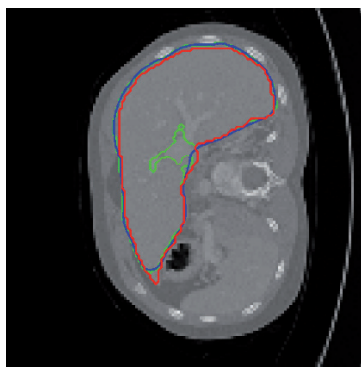


Fig. 15. Segmentation result using deformable surfaces (level set), using as a mask the initial segmentation. Red contour – ground truth, green contour - initialization mask, and blue contour – the segmentation result.

Contrast agent	Vol	Step 1	Step 2	Step 3	Step 1	Step 2	Step 3
		<i>Sn</i>	<i>Sn</i>	<i>Sn</i>	<i>VO_E</i>	<i>VO_E</i>	<i>VO_E</i>
no	1	0.94	0.95	0.96	13.1%	12.1%	11.1%
no	2	0.90	0.93	0.95	13.56%	11.33%	10.53%
no	3	0.90	0.91	0.97	13.87%	11.38%	8.02%
yes	4	0.94	0.95	0.97	15.02%	13.80%	13.01%
yes	5	0.90	0.91	0.93	12.83%	12.43%	11.73%
yes	6	0.95	0.94	0.94	14.08%	13.13%	12.58%
yes	7	0.90	0.92	0.96	14.47%	13.47%	13.1%
yes	8	0.90	0.91	0.96	11.96%	11.81%	8.8%
yes	9	0.79	0.89	0.95	24.1%	13.81%	10%

Tab. 5. Segmentation evaluation after each step.

Contrast agent	Vol	<i>Sn</i>	<i>Sp</i>	Error Rate	<i>Acc</i>	<i>Diff_V</i>	<i>VO_E</i>
no	1	0.96	0.99	0.6%	99.5%	1.4	11.1%
no	2	0.95	0.99	0.55%	99.80%	1.03	10.53%
no	3	0.97	0.99	0.41%	99.72%	3	8.02%
yes	4	0.97	0.99	0.64%	99.44%	4.6	13.01%
yes	5	0.93	0.99	0.73%	99.88%	-2.3	11.73%
yes	6	0.95	0.99	0.55%	99.63%	4.39	12.58%
yes	7	0.96	0.99	0.65%	99.77%	7.9	13.1%
yes	8	0.96	0.99	0.44%	99.90%	1.86	8.8%
yes	9	0.95	0.99	0.42%	99.75%	1.39	10%

Tab. 4. Segmentation evaluation after applying active contours (deformable surfaces).

An additional table summarizing the results in terms of specificity, sensitivity and volumetric overlap error after each of the three segmentation steps shown in Fig. 1 (namely, Tab. 5) was added, to allow noticing the sometimes slight improvement, but in some cases significant improvement in the performance – e.g., in the volumetric overlap error, which (for example, in the case of the 3rd line in the table) decreases from 13.87% (automatic segmentation) to 11.38% (manual refinement) and 8.02% (after applying level set segmentation). The conclusion can be that, while not always necessary, the two refinement steps may be in some cases very useful mandatory.

The results are promising and advantages of the proposed approach are evident and include basic tools for segmentation and refinement/editing, all working in 3D space making both interaction and computation faster than in 2D space.

Regarding the segmentation algorithm, the most important advantage is the short convergence time (10 min – taking into account that the algorithms was developed in Matlab, shorter convergence time can be obtained when the algorithm is developed in a faster programming language as C, C++)(thanks to the proposed solution that works at 3D block level instead of pixel level).

Regarding editing/segmentation system, the principal advantage is that it can easily be integrated with actual workflow and with reduced costs less hardware demanding and present less complexity compared with Liver Planer [22] that is one of the few existing solutions that are available for this purpose of 3D segmentation/refinement and that actually use real 3D interaction tools and not only transformations/mapping of 2D interaction tools in 3D scene/space.

6. Conclusions

This paper proposes and evaluates a promising system used for liver segmentation that can be used as the first step in liver treatment planning. It is based on texture feature analysis obtained from 3D DCT block coefficients, support vector machines, and refinement provided by combined morphological operations, median filtering and connected components. Further refinement is necessary in certain cases despite the good accuracy of the automatic segmentation, due to inter and even intra-patient variability inside the liver parenchyma, limited resolution of the CT scans and possible acquisition artifacts. Immersive interaction alleviates many interpretation and visualization problems enabling the clinicians to have a more natural view of the medical data represented as a 3D volume. That is why we provided a 3D tool for manual rough refinement of the initial segmentation result in the form of a flexible virtual 3D probe for manual interaction, using neuro-fuzzy techniques for two cameras. When more cameras are necessary, the fuzzy model can be easily extended by including a richer set of rules. Eventually, a fine refinement procedure based on 3D level sets is used for obtaining an accurate segmentation. The entire segmentation process was conducted at a 3D level (classification, post processing and also the refinement step) resulting in fewer connectivity errors and, due to the block-level supervised approach, faster computation time than existing 2D approaches. The obtained results on real CT volumes have demonstrated efficiency of the proposed approach. In our future work, we will investigate the possibility of generalizing the proposed framework for different imaging modalities and organ segmentation tasks, to create a flexible and easy to use and train 3D segmentation environment. Another proposed extension of our solution consists in its application on a 3D representation based on JPEG compressed CT slices, which can improve even further the computational efficiency of the segmentation. Further developments in the sense of multi-modal volumes segmentation will also be considered.

Acknowledgements

This paper was supported by the projects:

- "Doctoral studies in engineering sciences for developing the knowledge based society", SIDOC contract no. POSDRU/88/1.5/S/60078, project co-funded from European Social Fund through Sectorial Operational Program Human Resources 2007-2013;

- "Development and support of multidisciplinary postdoctoral programmes in major technical areas of national strategy of Research - Development - Innovation", 4D-POSTDOC, contract no. POSDRU/89/1.5/S/52603, project co-funded by the European Social Fund through Sectorial Operational Programme Human Resources Development 2007-2013.

References

- [1] LEE, J., KIM, N., LEE, H., SEO, J. B., WON, H. J. Y., SHIN, M. Efficient liver segmentation using a level-set method with optimal detection of the initial liver boundary from level-set speed images. *Computer Methods and Programs in Biomedicine*, 2007, vol. 88, p. 26–38.
- [2] SADDI, K. A., ROUSSON, M., CHEFD'HOTEL, C., CHERIET, F. Global-to-local shape matching for liver segmentation in CT imaging. In HEIMANN, T., STYNER, M., VAN GINNEKEN, B. (Eds.): *3D Segmentation in the Clinic: A Grand Challenge*, 2007, p. 207–214.
- [3] WIMMER, A., SOZA, G., HORNEGGER, J. Two-stage semi-automatic organ segmentation framework using radial basis functions and level sets. In *3D Segmentation in the Clinic: A Grand Challenge, MICCAI Workshop*. Springer, 2007, p. 179–188.
- [4] BEICHEL, R., BAUER, C., BORNIK, A., SORANTIN, E. Liver segmentation in CT data: A segmentation refinement approach. In *Proc. MICCAI Workshop 3-D Segmentat. Clinic: A Grand Challenge*, 2007, p. 235.
- [5] BECK, A., AURICH, V. HepaTux – A semiautomatic liver segmentation system. In HEIMANN, T., STYNER, M., VAN GINNEKEN, B. (Eds.): *3D Segmentation in the Clinic: A Grand Challenge*, 2007, p. 225–233.
- [6] ZHENG, Y., YANG, X., YE, X. Fully automatic segmentation of liver from multiphase liver CT. San Diego (USA), *Proc. SPIE* 6512, 2007.
- [7] SEO, K. S., KIM, H. B., PARK, T., KIM, P. K., PARK, J. A. Automatic liver segmentation of contrast enhanced CT images based on histogram processing. In *First International Conference Advances in Natural Computation ICNC 2005*. Changsha (China), p. 1027-1030.
- [8] RATHORE, S., IFTIKHAR, M. A., HUSSAIN, M., JALIL, A. Texture analysis for liver segmentation and classification: A survey. In *Frontiers of Information Technology (FIT)*, Dec.19-21, 2011, p.121-126,
- [9] CAMPADELLI, P., CASIRAGHI, E., LOMBARDI, G. Automatic liver segmentation from abdominal CT scans. In *Proceedings of the 14th International Conference on Image Analysis and Processing*, 2007, p. 731-736.
- [10] FURUKAWA, D., SHIMIZU, A., KOBATAKE, H. Automatic liver segmentation based on maximum a posterior probability estimation and level set method. In *Proc. MICCAI Workshop on 3-D Segmentat. Clinic: A Grand Challenge*, 2007.
- [11] RIKXOORT, E., ARZHAIEVA, Y., GINNEKEN, B. Automatic segmentation of the liver in computed tomography scans with voxel classification and atlas matching. In *Workshop on 3D Segmentation in the Clinic: A Grand Challenge, MICCAI 2007*, Brisbane (Australia).
- [12] ZHOU, X., KITAGAWA, T., OKUO, K., HARA, T., FUJITA, H., YOKOYAMA, R., KANEMATSU, M., HOSHI, H. Construction of a probabilistic atlas for automated liver segmentation in non-contrast torso CT images. *International Congress Series*, 2005, vol. 1281, p. 1169-1174.
- [13] LEE, J., KIM, N., LEE, H., SEO, J. B., WON, H. J., SHIN, Y. M., SHIN, Y. G., KIM, S. Efficient liver segmentation using a levelset method with optimal detection of the initial liver boundary from level-set speed images. *Compute Methods Programs Biomed*, Oct, 2007, vol. 88, no. 1, p. 26-38.
- [14] SEOL, Y., YU, J., KANG, T., CHOI, K., KIM, H., KIM, M. Resolving the initial contour problem of GVF snake in the sequential images. In *Conf. Proc. IEEE Eng Med Biol Soc*, 2007, p. 779-782.

- [15] OKADA, T., SHIMADA, R., SATO, Y., HORI, M., NAKAMOTO, M., CHEN, Y. W., NAKAMURA, H. Automated segmentation of the liver from 3D CT images using probabilistic atlas and multilevel statistical shape model. *Academic Radiology*, Nov. 2008, vol. 15, no. 11, p. 1390-1403.
- [16] VARMA, J., DURGAN, J., SUBRAMANYAN, K. Semi-automatic procedure to extract continued liver segments from multislice CT data. San Diego, (CA, USA), p. 561-568, 2003.
- [17] GRATZEL, C., FONG, T., GRANGE, S., BAUR, C. A Non-contact mouse for surgeon-computer interaction. *Technology and Health Care Journal*, IOS Press, 2004. vol. 12.
- [18] FEIED, C., GILLAM, M., WACHS, J., HANDLER, J., STERN, H., SMITH, M. A real-time gesture interface for hands-free control of electronic medical records. In *AMIA Annual Symposium Proceedings*. Washington (DC, USA), February 2006.
- [19] PAOLIS, L., PULIMENO, M., ALOISIO, G. Advanced visualization and interaction systems for surgical pre-operative planning. *Journal of Computing and Information Technology*, 2010, vol. 18, no 4, p. 385-392.
- [20] GALLO, L., CIAMPI, M. Wii remote-enhanced hand-computer interaction for 3D medical image analysis. In *International Conference on Current Trends in Information Technology CITT 2009*. 2009, p. 85- 90.
- [21] COOPERSTOCK, J. R., WANG, G. Stereoscopic display technologies, interaction paradigms, and rendering approaches for neurosurgical visualization. In *Stereoscopic Displays and Applications*. San Jose (CA, USA), January 2009.
- [22] REITINGER, B., BORNICK, A., BEICHEL, R., SCHMALSTIEG, D. Liver surgery planning using virtual reality. *IEEE Computer Graphics and Applications*, Nov./Dec. 2006, vol. 26, no. 6, p. 36 to 47.
- [23] POPA, C., GORDAN, M., VLAICU, A., ORZA, B., OLTEAN, G. Computationally efficient algorithm for fuzzy rule-based enhancement on JPEG compressed color images. *WSEAS Transactions on Signal Processing*, May 2008, vol. 4 no. 5, p. 310 -319.
- [24] MALCOLM, J., RATHI, Y., YEZZI, A., TANNENBAUM, A. Fast approximate surface evolution in arbitrary dimension. In *Proc. SPIE Medical Imaging 2008: Image Processing*. 2008 February, 6914.
- [25] JIANG, C., ZHANG, X., MEINEL, C. Hybrid framework for medical image segmentation. In *Proceedings of the 11th International Conference on Computer Analysis of Images and Patterns (CAIP'05)*. Springer-Verlag, Berlin, Heidelberg, 2005, p. 264-271.
- [26] PENNEBAKER, W. B., MITCHELL, J. L. *JPEG: Still Image Compression Standard*. New York: Van Nostrand Reinhold, 1993.
- [27] JIANG, J., FENG, G. The spatial relationship of DCT coefficients between a block and its sub-blocks. *IEEE Transactions on Signal Processing*, May 2002, vol. 50, no. 5, p.1160-1169.
- [28] PUN, C. M., ZHU, H. M. Textural image segmentation using discrete cosine transform. In *Proceedings of the 3rd International Conference on Communications and Information Technology*. Greece, December 2009.
- [29] SGOUROS, N., SANGRIOTIS, M., MAROULIS, D. Multiview image compression: future challenges and today's solutions. In *1st International Scientific Conf. eRA T.E.I of Piraeus & University of Paisley*. Tripoli, Sept. 16-17, 2006.
- [30] CHAN, R. K. W., LEE, M. C. 3D-DCT quantization as a compression technique for video sequences. In *International Conference on Virtual Systems and MultiMedia, VSMM*. 1997, p. 188.
- [31] VAPNIK, V. N. *Statistical Learning Theory*. New York: Wiley, 1998.
- [32] LIN, C. J., WENG, R. C. Probability estimates for multi-class classification by pair wise coupling. *The Journal of Machine Learning Research archive*, 2004, vol. 5.
- [33] PLATT, J. Probabilistic outputs for support vector machines and comparisons to regularized likelihood methods. In *Advances in Large Margin Classifiers* (Smola, A., Bartlett, P., Scholkopf, B., Schuurmans, D., Eds.). Cambridge (England, MA): MIT Press, 2000.
- [34] DANCIU, M., GORDAN, M., ORGHIDAN, R., SORANTIN, E., FLOREA, C., VLAICU, A. A fuzzy logic-guided virtual probe for 3D visual interaction applications. In *IEEE International Conference on e-Health and Bioengineering (EHB 2011)*. Iasi (Romania), 24-26 November, 2011, p. 431- 434. ISBN: 978-606-544-078-4.
- [35] CHIH-CHUNG CHANG, CHIH-JEN LIN LIBSVM, A library for support vector machines. *ACM Transactions on Intelligent Systems and Technology*, 2011. [Online] Software available at <http://www.csie.ntu.edu.tw/~cjlin/libsvm>.
- [36] CIECHOLEWSKI, M., OGIELA, M. R. Automatic segmentation of neoplastic hepatic disease symptoms in CT images. In *Proceedings of the 4th International Conference on Modeling Decisions for Artificial Intelligence*. Kitakyushu (Japan), 2007, p. 414-421.
- [37] CAMPADELLI, P., CASIRAGHI, E., PRATISSOLI, S. Fully automatic segmentation of abdominal organs from CT images using fast marching methods. In *Proceedings of the 2008 21st IEEE International Symposium on Computer-Based Medical Systems*, 2008, p. 554-559.
- [38] XU, D., LEE, J., RAICU, D. S., FURST, J. D., CHANNIN, D. Texture classification of normal tissues in computed tomography. In *The 2005 Annual Meeting of the Society for Computer Applications in Radiology*, June 2-5, 2005.
- [39] FORUZAN, A., AGHAEIZADEH, R., HORI, M., SATO, Y. Liver segmentation by intensity analysis and anatomical information in multi-slice CT images. *International Journal of Computer Assisted Radiology and Surgery*, 2009, vol. 4, no. 3, p. 287-297.
- [40] YUSSOF, W., BURKHARDT, H. 3D liver segmentation using hybrid segmentation techniques. In *Proceedings of the International Conference of Soft Computing and Pattern Recognition*, 2009, p. 404-408.
- [41] LUO, S., JIN, J. S., CHALUP, S. K., QIAN, G. A liver segmentation algorithm based on wavelets and machine learning. In *International Conference on Computational Intelligence and Natural Computing CINC'09*. Wuhan (China), 2009, vol. 2, p. 122-125.

About Authors

Marius DANCIU, born in 1984, received the B.Sc. and the Ph.D. degrees in Electronics and Telecommunications Engineering, from the Technical University of Cluj-Napoca (TUCN), Romania, in 2008 and 2012, respectively. He is currently a collaborator of the Multimedia Technologies and Telecommunications Research Centre at the Dept. of Communication, Faculty of Electronics, Telecommunications and Information Technology, TUCN. His research interests are: 3D image processing and analysis, medical imaging, 3D interactive tools, DICOM technologies.

Mihaela GORDAN, born in 1971, received the Ph.D. degree in Electronics and Telecommunications Engineering and the B.Sc. degree in Applied Electronics Engineer

ing in 2004, and 1995, respectively, from the Technical University of Cluj-Napoca (TUCN), Romania. Currently, she is an Associate Professor at the Dept. of Communication, Faculty of Electronics, Telecommunications and Information Technology, TUCN. She is an expert in digital image processing and analysis, multimodal image analysis, fuzzy logic, fuzzy image processing and machine learning for image analysis and understanding.

Camelia FLOREA, born in 1981, received the B.Sc. and Ph.D. degrees in Electronics and Telecommunications Engineering in 2005, and 2009, respectively, from the Technical University of Cluj-Napoca, Romania. Currently, she is an Assistant Professor at the same university, in the Dept. of Communication, Faculty of Electronics, Telecommunications and Information Technology. Her research interests are: signal processing and analysis, images and video sequences compression, compressed domain data processing, multimedia technologies, artificial intelligence and fuzzy logic.

Radu ORGHIDAN, born in 1977, received the Ph.D. degree in Information Technologies from the University of Girona, Spain, and the B.Sc. degree in Automation and Informatics Engineering from the Technical University of Cluj-Napoca (TUCN), Romania, in 2006, and 2001, respectively. Currently, he is a postdoctoral researcher in the computer vision field at the TUCN. His research is focused on 3D perception using stereoscopic techniques, 3D inter-

active tools, image processing, multimedia technologies and eLearning.

Erich SORANTIN was born in 1957. After finishing the high school in 1976 he studied medicine at the University of Vienna. Promovation was in March 1982. His scientific interest was always targeted in biosimulation, expert systems and image processing. Papers and congress contributions were dealing with expert systems for mechanical ventilation in newborns, automated detection of breast cancer in digitized mammographies breast xray images and the application of Virtual Reality in Radiology including virtual endoscopy. He is now the head of research unit for digital information and image processing and also professor at the Division of Pediatric Radiology at Medical University of Graz.

Aurel VLAICU, born in 1950, received the Ph.D. degree in Electronics and Telecommunications Engineering from the Technical University of Cluj-Napoca (TUCN), Romania, and the B.Sc. degree in Radiocommunications Engineering from "Politehnica" University of Bucharest, Romania, in 1994, and 1974, respectively. He is a Professor at the Dept. of Communication, Faculty of Electronics, Telecommunications and Information Technology, TUCN, and in 2012 he became the rector of the TUCN. He is an expert in digital image processing and analysis, images and video sequences compression, television, multimedia technologies, and eLearning.